energies

MDPI

Article

The Feasibility of Improving the Accuracy of In Situ Measurements in the Air-Surface Temperature Ratio Method

Seo-Hoon Kim [1,2], Jung-Hun Lee [1,3], Jong-Hun Kim [1,*], Seung-Hwan Yoo [1] and Hak-Geun Jeong [1]

[1] Energy ICT·ESS Laboratory, Korea Institute of Energy Research, Daejeon 34101, Korea; takesky@kier.re.kr (S.-H.K.); junghun@kier.re.kr (J.-H.L.); shyoo@kier.re.kr (S.-H.Y.); hgjeong@kier.re.kr (H.-G.J.)
[2] Department of Architectural Engineering, Hanyang University, Seoul 04763, Korea
[3] Department of Architectural Engineering, Sungkyunkwan University, Suwon 16419, Korea
* Correspondence: jonghun@kier.re.kr; Tel.: +82-42-860-3467

Received: 15 June 2018; Accepted: 16 July 2018; Published: 19 July 2018

Abstract: This paper reports on a feasibility study conducted to improve the in situ measurement accuracy of the air-surface temperature ratio (ASTR) method. The measured relative error rate was analyzed using the ISO 6946 [7.69 W/(m^2·K)] and Korea Energy Saving Design Standard [9.09 W/(m^2·K)] indoor total surface heat transfer coefficients. The relative error rate was analyzed according to fluctuations in outdoor temperature data. The relative error rate obtained using the ISO 6946 standard was analyzed about 6.3% and that obtained using the Korea Energy Saving Design Standard was about 9.5%. The relative error rate measured for outdoor temperature fluctuations of less than 1 K was about 4.62% and that for temperatures greater than 1 K was about 14.31%. The study results confirmed the cause of the error in the measurement of the ASTR. It was also found that the accuracy of the latter can be improved when the ISO 6946 indoor total surface heat transfer coefficient is applied and when outdoor temperature fluctuations less than 1 K are sampled and analyzed.

Keywords: air-surface temperature ratio; indoor total surface heat transfer coefficient; in situ measurement of U-value

1. Introduction

Korea has taken measures to reduce energy consumption and greenhouse gas emissions from buildings. The Korean government has announced amendments including those related to greenhouse gas reduction and strengthening of the insulation of building envelope, to the Energy Saving Design Standards [1]. However, these amendments are limited to new buildings; hence, the range of energy savings is limited. According to the European Union directive 2012/27/EU [2], existing buildings have the greatest potential for saving energy [3]. In fact, it is more necessary to reduce CO_2 emissions from existing buildings than from new buildings [4,5]. There is, in particular, a need for measures to improve the energy efficiency of deteriorated houses with high energy losses [6].

The energy efficiency of these deteriorated houses can be improved through retrofitting [7]. However, pre-work is required for this. The energy performance of existing buildings must be analyzed by measuring the insulation performance of the deteriorated houses in them. One of the most important parameters in calculating building energy demand in the retrofit design phase is the value of energy lost through the building envelope. It is particularly important to quantitatively calculate the U-value of the building envelope [W/(m^2·K)].

However, it is very difficult to estimate the wall insulation performance of a deteriorated building. Therefore, in analyses of the energy performance of a building, the U-value generally uses the initial data or the estimated U-value of the building design stage. The initial U-value of the design and related estimates differ from the actual (measured) U-value. This difference has a great impact on the energy performance of buildings. Therefore, a method to precisely diagnose the U-value of the envelopes of deteriorated house is required. The following are the three most common approaches for in situ measurement of the U-value of a building envelope:

1. The ISO 9869-1: 2014 [8] international standard heat flow meter (HFM) method: This measures the U-value in situ using the heat flux of the building envelope and the temperature difference between the indoor and outdoor environments. The average method is one of those most commonly used to evaluate the thermal properties of building elements using in situ measurements [9]. The U-value is measured under quasi-steady state conditions [10–15]. However, the latter are difficult to measure and thus the average heat flow of the building envelope must be measured for a sufficiently long time. The ISO 9869-1: 2014 standard requires data sampling to last for at least three to seven days. It is common for the monitoring period to extend to more than two weeks to achieve satisfactory results and stable conditions [16].
2. Theoretical calculation using the ISO 6946: 2007 standard [17]: This method is based on calculations of thermal resistance and heat transfer rate of doors, windows, and other building components. The calculation is based on an appropriate design thermal conductivity or design thermal resistance of the material. It is applied to a component composed of a thermally homogeneous layer and takes into account the thickness and thermal conductivity of each layer making up the envelope. Thermal conductivity is calculated according to ISO 10456 [18]. However, this method is approximate and the U-value obtained differs from the actual value.
3. Using infrared cameras: This approach uses the infrared thermovision technique (ITT) [19–22] to analyze the surface temperature of the envelope. The U-value of the building envelope can be calculated using the temperature information and the total heat transfer coefficient. A standard is currently being established for ISO 9869-2 [23].

Among the above, the HFM method is the most accurate [24–26]. However, this method takes 7 to 14 days for heavy structures and data collection takes at least 3 days. Previous studies [10–15] using the HFM method measured the U-value of the building envelope over a long period of seven days or longer. In other words, it does not provide a means to measure the thermal performance of a building over a short period of time. For this reason, previous studies have proposed the air-surface temperature ratio (ASTR) method [27], which can overcome the disadvantages of the current measurement methods [28]. An appropriate measurement period was also calculated to satisfy the measurement conditions. The ASTR method uses simple and rapid measurements compared to other in situ thermal p erformance measurement methods. A previous study [27] confirmed the possibility of measuring the U-value of a building over a short period of time. However, ensuring measurement accuracy was very difficult; valid measurement values were obtained only when the measurement conditions were satisfied. In addition, the previous study [27] found that it takes a long time to implement the measurement conditions and analyze the data. Therefore, this study examined the problems raised in the previous research and analyzed the variables affecting the measurement accuracy. In addition, this study proposes a method to improve measurement accuracy by analyzing the factors causing the relative error rate in the ASTR method. During the study, in situ measurements of the thermal performance of residential buildings were performed using the wall U-value metering system with the ASTR method.

2. Method

2.1. Study Process

Figure 1 shows a process flowchart for this study. First, the thermal performance of in situ measurement methods (ISO 9869-1 HFM method, ISO 6946 method of calculating thermal resistance and heat transfer, and ISO 9869-2 ITT method) was studied and their advantages and disadvantages were analyzed. Secondly, the ASTR method for in situ measurement of U-values is described, including how it proposed measuring the wall U-value by the multiplying indoor total surface heat transfer coefficient by the indoor and outdoor temperature differences, indoor air temperatures, and wall surface temperature differences. Thirdly, the buildings, measurement equipment and measurement conditions are described and the study outlined. The U-value was measured by applying the ISO 9869-1 HFM and ASTR methods to target houses. These methods were compared to verify the relative error rate of the measurements. Fourthly, analysis of the measured relative error rates and accuracy based on the indoor total surface heat transfer coefficients and outdoor temperature fluctuations are presented. Finally, a way for improving the accuracy of in situ measurement of ASTR method is suggested.

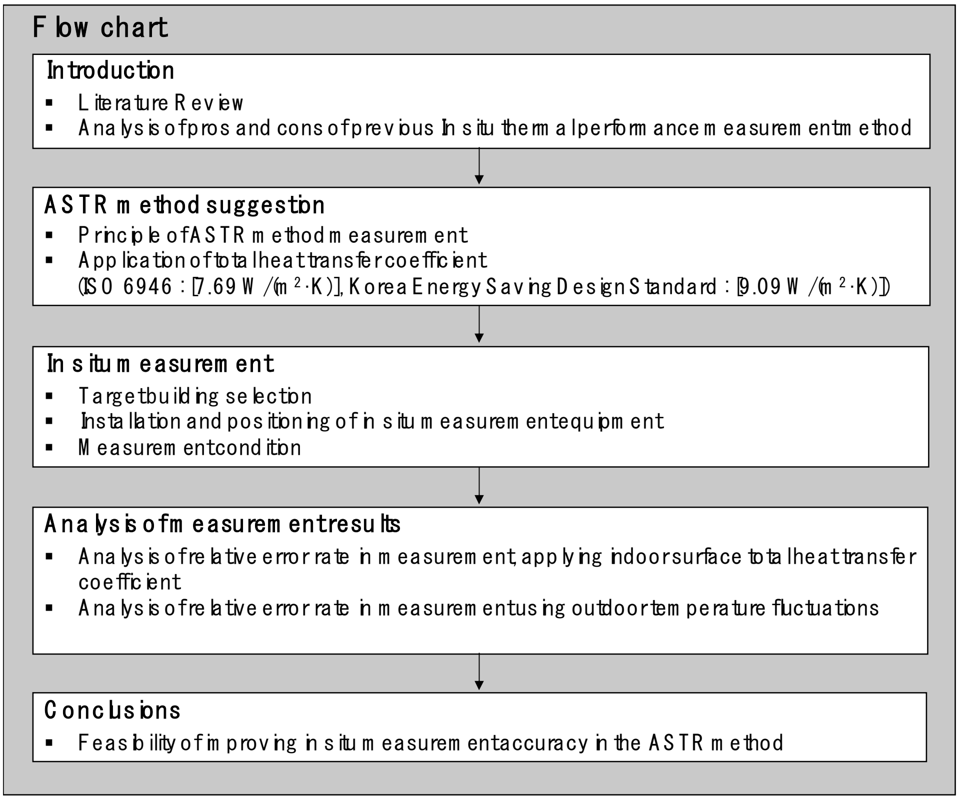

Figure 1. The study process.

2.2. The Air-Surface Temperature Ratio (ASTR) Method

The ASTR method was devised by applying the above concept [29]. The ASTR method assumes a quasi-steady state in which heat loss through radiation and convective heat transfer from the wall surface into the room is equal to that from conduction through the wall. Furthermore, the heat loss through radiation and convective heat transfer from the outdoor wall surface into the room is equal to that through the heat transfer by conduction through the wall. The following formulas represent the ASTR method, and the concept is illustrated in Figure 2:

$$\begin{aligned} \mathrm{q} &= h_{t,i}\left(t_{i,air} - t_{i,surface}\right) = \tfrac{k_1}{b_1}(t_{i,\mathrm{surface}} - t_{1,2}) = \tfrac{k_2}{b_2}(t_{1,2} - t_{2,3}) \\ &= \tfrac{k_3}{b_3}(t_{2,3} - t_{3,4}) = h_{t,e}\left(t_{e,surface} - t_{e,air}\right) \end{aligned} \quad (1)$$

$$t_{i,air} - t_{i,surface} = q\tfrac{1}{h_{t,i}},\ t_{i,surface} - t_{1,2} = q\tfrac{b_1}{k_1},\ t_{1,2} - t_{2,3} = q\tfrac{b_2}{k_2},\ t_{2,3} - t_{3,4} = q\tfrac{b_3}{k_3},\ t_{3,4} - t_{e,surface} = q\tfrac{1}{h_{t,e}} \quad (2)$$

$$\sum \Delta t : t_{i,air} - t_{e,air} = q\left(\frac{1}{h_{t,i}} + \frac{b_1}{k_1} + \frac{b_2}{k_2} + \frac{b_3}{k_3} + \frac{1}{h_{t,e}}\right) \quad (3)$$

$$q = U \cdot A \cdot \Delta t = \frac{q}{\Delta t} = \frac{h_{t,i}\left(t_{i,air} - t_{i,surface}\right)}{\left(t_{i,air} - t_{e,air}\right)} \tag{4}$$

$$U = h_{t,i}\left[\frac{\sum_{j=1}^{n}\left(t_{i,air,j} - t_{i,surface,j}\right)}{\sum_{j=1}^{n}\left(t_{i,air,j} - t_{e,air,j}\right)}\right] \tag{5}$$

where q: heat flux [W/m^2], $t_{i,air}$: indoor air temperature, $t_{i,surface}$: indoor wall surface temperature, $t_{e,air}$: outdoor air temperature, k_n: wall element, b_n: wall thickness, t_n: surface temperature of the wall element, $h_{t,i}$: total indoor wall surface heat transfer coefficient [W/(m^2·K)], and $h_{t,e}$: total external wall surface heat transfer coefficient [W/(m^2·K)].

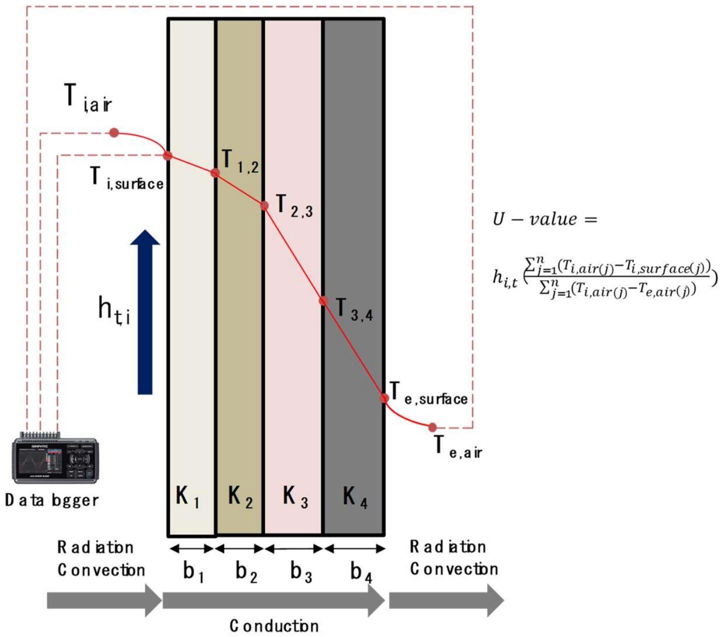

Figure 2. The air-surface temperature ratio (ASTR) method.

In the above equation, $h_{t,i}$ represents the indoor heat transfer coefficient; k_1, k_2, and k_3 represent the third layer from the first layer; and $h_{t,e}$ represents the outdoor heat transfer coefficient. Under quasi-steady state conditions, the heat flow q through the wall is constant, so the heat flow from the indoor to the outside remains the same. By applying this theory, the ASTR method calculates the U-value of a wall using the indoor surface total heat transfer coefficient; the values of the total heat transfer coefficient considering radiation and convection were used here. In this study, a surface resistivity of 0.13 m^2·K/W and a horizontal surface heat resistance of 0.10 m^2·K/W were used for the interior wall surface, as suggested by ISO 6946 (Building components and building elements–Thermal resistance and thermal transmittance–Calculation method) [30–33]. The reciprocal of these values was used to calculate the indoor total heat transfer coefficient (Vertical: 7.69 W/(m^2·K), horizontal: 10 W/(m^2·K)). The indoor total surface heat transfer resistance value proposed in the Korean Energy Saving Design Standard (2016) was also used [34]. In this study, the U-values of walls and roofs were derived by applying 0.11 m^2·K/W to vertical surface heat resistance and 0.086 m^2·K/W to horizontal surface heat transfer resistance (Vertical: 9.09 W/(m^2·K), horizontal: 11.63 W/(m^2·K)). The estimated and measured relative error rates were analyzed by comparing these results. The indoor surface total heat transfer coefficient varies depending on the in situ conditions and measurement conditions. In this study, the ratio of the convection heat transfer coefficient (4–5 W/(m^2·K)) and radiation heat transfer coefficient (3–4 W/(m^2·K)) was used as in Cholewa et al. [35]. Tables 1 and 2 show the indoor surface thermal resistance values given in the Korea Energy Saving Design Standard and in ISO 6946.

Table 1. Values of indoor and outdoor heat transfer resistance according to the Korean Energy Saving Design Standard.

Direction	Indoor Heat Transfer Resistance [$m^2 \cdot K/W$]	Outdoor Heat Transfer Resistance [$m^2 \cdot K/W$]	
		Indirect	Directly
Vertical	0.11	0.11	0.043
Horizontal (Ground floor)	0.086	0.15	0.043
Horizontal (Rooftop)	0.086	0.086	0.043

Table 2. Values for Heat transfer resistance according to ISO 6946.

Direction	Indoor Heat Transfer Resistance [$m^2 \cdot K/W$]	Outdoor Heat Transfer Resistance [$m^2 \cdot K/W$]
Vertical	0.13	0.04
Horizontal (Upward)	0.10	0.04
Horizontal (Downward)	0.17	0.04

3. Overview of U-Values In Situ Measurement of Residential Building Envelopes

3.1. Target Buildings

The target buildings were selected based on the standard housing models in the "Energy Efficiency Improvement Project of Low Income House" implemented by the Korean Energy Foundation in 2017 [36,37]. The target houses are located in Gimpo (latitude: 37.61° N, longitude: 126.71° E) and Hapcheon (latitude: 35.56° N, longitude: 128.16° E). The buildings were built between 1982 and 1994; thus, all four houses were 20 years old or more at the time of the study.

The in situ measurement period was about one month from 15 November 2017 to 15 December 2017. Cases A and B had a wall U-value of 0.636 W/($m^2 \cdot K$) and a roof U-value of 0.41 W/($m^2 \cdot K$) [38] when designed; Cases C and D had wall U-values of 1.162 W/($m^2 \cdot K$) and a roof U-value of 1.05 W/($m^2 \cdot K$). Photographs of the buildings are given in Figure 3. Tables 3 and 4 give an overview of the studied buildings and present their thermophysical properties at initial design, respectively.

Table 3. Overview of the studied buildings.

Classification	Case A	Case B	Case C	Case D
Location	Gimpo	Gimpo	Hapcheon	Hapcheon
Completion Date	1994	1988	1982	1983
Floor Area	99.1 m^2	36.1 m^2	78.0 m^2	70.0 m^2
Ceiling Height	2.3 m	2.3 m	2.7 m	2.3 m
Orientation	South	South	South	South

Table 4. Thermophysical properties at initial design.

Classification		#	Component	d (mm)	λ [W/(m·K)]	R [$m^2 \cdot K/W$]
Initial Design U-value	Cases A and B	1	Indoor surface heat transfer resistance			0.13
		2	Cement mortar	20	1.4	0.0143
		3	Brick, cement	90	0.6	0.015
		4	Expanded polystyrene No. 1. 4	50	0.043	1.1628
		5	Brick, red	90	0.78	0.01154
		6	Outdoor surface heat transfer resistance			0.04
			U-value		0.620 [W/($m^2 \cdot K$)]	
		#	Component	d (mm)	λ [W/(m·K)]	R [$m^2 \cdot K/W$]
	Cases C and D	1	Indoor surface heat transfer resistance			0.13
		2	Cement mortar	20	1.4	0.0143
		3	Brick, cement	90	0.6	0.015
		4	Air gap	10		0.086
		5	Polyurethane (PUR)	10	0.028	0.3571
		6	Brick, cement	90	0.6	0.15
		7	Cement mortar	20	1.4	0.0143
		8	Outdoor surface heat transfer resistance			0.04
			U-value		1.062 [W/($m^2 \cdot K$)]	

(**a**) (**b**) (**c**) (**d**)

Figure 3. The target buildings: (**a**) Case A; (**b**) Case B; (**c**) Case C; (**d**) Case D.

3.2. In Situ Measurement Equipment

Table 5 shows the equipment used to measure the insulation performance of the walls of the buildings in this study. First, a TR-72wf hygrometer was installed in each room to measure temperature and humidity. Then the building envelope U-values were measured using the HFM [39–41] and ASTR methods. The heat flux (q) and indoor and outdoor temperatures ($T_{i,air}$ and $T_{e,air}$) were measured using a GreenTEG sensor, which ensured the accuracy and reliability of the measurement. The thermal performance of the wall was measured continuously for one week. Next, the ASTR method was evaluated using the developed U-value metering system. Using U-value metering system, the indoor-side wall surface temperature ($T_{i,surface}$), outdoor temperature ($T_{e,air}$), and indoor wall air temperature ($T_{i,air}$) data were obtained.

Table 5. Overview of measurement equipment.

Item	Classification		Accuracy	
HFM method	Model Quantity	G. Inc Heat Flux Kit 16 EA	Heat Flux (W/m^2) <0.22	Temperature (°C) ±0.5
ASTR method	Model Quantity	U-value metering system Hub 4 EA Sensor 32 EA	–	Temperature (°C) ±0.5
Wall surface temperature & gradient	Model Quantity	F. Inc IR camera 1 EA		Temperature (°C) ±2., 2%
Air Temperature & humidity (Reference)	Model Quantity	T. Inc_TR-72wf 4 EA	Humidity (%) ±5 RH	Temperature (°C) ±0.5

In the ASTR method, the U-value metering system consists of one hub and eight wireless sensors developed by Korea Institute of Energy Research (KIER). The hub is capable of receiving data from a wireless temperature sensor through Bluetooth at five min intervals.

The wireless temperature measurement sensor measured the surface temperature of the wall with an infrared (IR) sensor, measured the room temperature and humidity, and transmitted the results to the hub. The wall U-value metering module systems measured the wall U-values within a short time at a low equipment cost. Each of the heat flow and ASTR wall U-value metering system sensors were installed at one point on each wall and one point on the surface of the roof (wall: four points, roof: one point). The installation is shown in Figure 4.

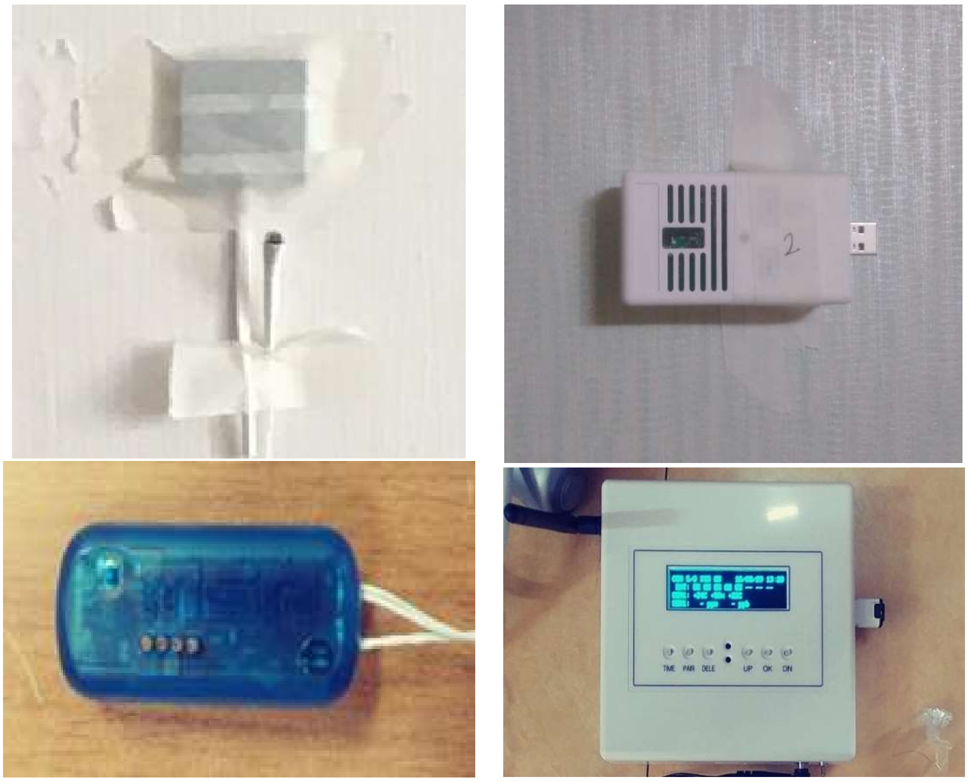

(**a**) (**b**)

Figure 4. Installed in situ measurement equipment for calculations using the (**a**) heat flow meter and (**b**) the air-surface temperature ratio.

3.3. In Situ Measurement Conditions

It was important that the ASTR method measurements were performed in an environment in which the indoor and outdoor environmental conditions were similar to the quasi-steady state. In these conditions, the flow direction of the indoor wall must be kept in one direction, i.e., from indoor to outdoor (or outdoor to indoor) according to time. In addition, it is difficult to take ASTR measurements under conditions of sudden temperature changes. Therefore, the following measurement conditions were required to remain constant:

(1) The heat flux of the building envelope.
(2) The variation in the indoor temperature.
(3) The variation in the outdoor temperature.

It was necessary to select a time and time zone in which the aforementioned conditions were satisfied, with a minimal change in the temperature between the time and time zone. The outdoor air temperature should not differ from the original temperature at the start of the test by more than ±10 °C, for at least 24 h before the start of the test [42,43].

The following measurement procedures and conditions were applied to measure the wall U-value: first, the sensor installation position was selected by referring to the ISO 6781 standard [44], and these criteria were used to find the appropriate sensor installation position (excluding cracks, thermal bridges, and corners of the wall) was found using an infrared camera. The sensor was placed at a representative location of the wall to measure the temperature. The in situ measurements were not conducted if the wall surface was wet, or if it rained during the test period, or if the wind speed exceeded 8 m/s. The sensor was installed in a location that was not directly affected by the location of a heater, cooler, or fan. If an outdoor wall or window was to be measured, a structure with an artificial shield and a barrier that protected it from rain, snow, direct solar radiation, among other factors, was needed (measuring the indoor side wall is recommended). The experimental conditions were considered to be in the quasi-steady state when the indoor temperature varied in the range of 0.1 °C to 0.4 °C and the outdoor temperature variation was less than 1 °C. In this study, we selected the time between 2:00 to 6:00 a.m. to implement the quasi-steady state conditions. The data were measured in 5 min intervals. The indoor air temperature was set at 18–20 °C and the indoor and outdoor temperature differences measured ranged from 10–15 °C. The U-value was calculated using the metering system developed in this study under the above measurement conditions.

The measurements were performed taking the above conditions into consideration, and four experimental results were derived by applying the following experimental conditions:

(1) Applied heat transfer coefficient of the indoor side wall and horizontal surface (based on ISO 6946).
(2) Applied heat transfer coefficient of the indoor side wall and horizontal surface (based on the Korea Energy Saving Design Standard).
(3) No data sampling in sections where the change in outdoor temperature was large.
(4) Sampling data where a satisfactory range in the differences in outdoor temperature difference were present (outdoor temperature fluctuations: less than 1 °C).

4. Results and Discussion

This study was conducted to quantitatively measure the U-value of walls of deteriorated houses. The HFM and ASTR methods were applied to analyze the thermal performance of the walls and roofs of residential buildings. Using these methods, it was possible to quantitatively analyze the insulation performance of residential buildings over 20 years old. In addition, the accuracy and relative error rate of the in situ measurement method were verified by comparing the results to those of the HFM and ASTR methods.

The measurement results were first analyzed using the indoor total surface heat transfer coefficients of the Korean Energy Saving Design and ISO 6946 standards. Then the measurement results were compared and analyzed based on the presence or absence of samples taken under the appropriate measurement conditions (outdoor temperature fluctuations).

4.1. Application of Indoor Total Surface Heat Transfer Coefficient

The wall and roof U-values of the target residential buildings were measured using the ISO 9869-1 HFM and ASTR methods. In the case of the ASTR method, the indoor total surface heat transfer coefficient was analyzed using two criteria: the Korean standard and the ISO 6946 standard. The measured relative error rate was analyzed by comparing the results of the HFM method with that of the U-value applied to the indoor-side wall heat transfer coefficient standards. The U values of the field measurements, according to the application of the total surface heat transfer coefficient, are shown in U_{HFM} in Table 6.

The U-value derived from the HFM method and the U-value results derived from U_{ASTR_1} and U_{ASTR_2} are also shown in Table 6. In addition, Table 7 shows the results of the measured relative error percentages by applying the standard indoor total surface heat transfer coefficient. The thermal performance of all cases was lower than the thermal performance designed at the time of completion (Tables 3 and 4). The measured relative error rate of U_{ASTR_1} was less than that of U_{ASTR_2}. The method using the ISO 6946 indoor total surface heat transfer coefficient exhibited high measurement accuracy. However, the measured relative error rate was less than 10% in both cases and the error tolerance was satisfied. There were no large differences in the range of the error rate, but this may be a factor that influences the measurement accuracy.

Table 6. U-value in situ measurement result according to the application of the indoor total surface heat transfer coefficient. (**a**) U_{HFM} (ISO 9869); (**b**) U_{ASTR_1} (ISO 6946); (**c**) U_{ASTR_2} (Korea Energy Savings Design Standard).

Classification	Item	W1 (East)	W1 (West)	W1 (South)	W1 (North)	R1
U_{HFM} [W/(m^2·K)] (a)	Case A	–	–	1.333	1.328	1.088
	Case B	–	–	1.810	1.701	1.385
	Case C	2.155	2.148	2.121	2.266	1.578
	Case D	1.555	1.508	1.511	1.519	1.055
U_{ASTR_1} [W/(m^2·K)] (b) $h_{t,\,i,\,wall}$ *: 7.69 W/(m^2·K) $h_{t,\,i,\,roof}$ **: 10.00 W/(m^2·K)	Case A	–	–	1.238	1.214	1.012
	Case B	–	–	1.673	1.599	1.283
	Case C	1.985	1.979	1.913	2.091	1.458
	Case D	1.438	1.398	1.411	1.403	0.988
U_{ASTR_2} [W/(m^2·K)] (c) $h_{t,\,i,\,wall}$: 9.09 W/(m^2·K) $h_{t,\,i,\,roof}$: 11.63 W/(m^2·K)	Case A	–	–	1.449	1.421	1.177
	Case B	–	–	1.958	1.871	1.492
	Case C	2.323	2.316	2.239	2.447	1.696
	Case D	1.683	1.636	1.651	1.642	1.149

* $h_{t,\,i,\,wall}$: Total surface heat transfer coefficient for the indoor wall. ** $h_{t,\,i,\,roof}$: Total surface heat transfer coefficient for the indoor roof.

Table 7. Measured relative error rate results of U_{HFM} and U_{ASTR}.

Classification	Item	W1 (East)	W1 (West)	W1 (South)	W1 (North)	R1
U_{HFM}~U_{ASTR} Relative Error factor (%)	Case A	–	–	7.13 *	8.58 *	6.99 *
		–	–	8.69 **	6.99 **	8.18 **
	Case B	–	–	7.57	6.00	7.36
		–	–	8.18	10.02	7.73
	Case C	5.97	6.74	4.87	4.43	4.20
		10.05	9.15	11.33	11.85	11.41
	Case D	6.20	6.74	5.87	5.71	6.35
		9.78	9.15	10.16	10.35	8.91

* $h_{t,\,i,\,wall}$: 7.69 W/(m^2·K), $h_{t,\,i,\,roof}$: 10.00 W/(m^2·K)—ISO 6946 Standard. ** $h_{t,\,i,\,wall}$: 9.09 W/(m^2·K), $h_{t,\,i,\,roof}$: 11.63 W/(m^2·K)—Korean Energy Saving Design Standard.

4.2. Data Sampling Based on Fluctuations in Outdoor Temperature

In the ASTR method, measurements should be conducted in an environment where the indoor and outdoor environmental conditions are similar to stable conditions (Section 3.3). This is because of the time required for the measurement condition (steady state or quasi-steady state) to stabilize (the time taken to reach the quasi-steady state).

The thermal performances and thermal resistance values of each structural property were different and varied widely. Therefore, a method for estimating the period during which the measurement condition was maintained in a steady or quasi-steady state was required. It was very difficult to maintain steady-state conditions under the actual conditions. Therefore, in this study, it was assumed that the experimental conditions were the quasi-steady state. To achieve this state, the room temperature was kept constant at 18–20 °C (using a radiant floor heating system). The measurements were taken from 2:00 to 6:00 a.m., during which the heat accumulation factor and solar radiation are not affected by the building envelope. The data were measured continuously over seven days and analyzed to achieve quasi-steady state conditions. Then data from the section where the outdoor temperature fluctuations were constant and those from sections where they were not were sampled and classified into six sections (six days of data). These data satisfy the measurement conditions proposed in Section 3.3 (constant temperature and measurement conditions are met). The procedure for analyzing the relative error from data sampling was as follows:

First, the heat flux was measured when outdoor temperature varied greatly in the quasi-steady state indoor condition. Next, the measurements were conducted in a section where the outdoor temperature did not vary as much. The results from the two measurement conditions were compared and analyzed. The measurement accuracy and measured relative error rate were analyzed using these measurement results. Figure 5 shows the fluctuations in outdoor temperature and the outdoor temperature data for each residential building in approximately six sections (data from 2:00 to 6:00 a.m.). The data were sampled per interval and the U-values were analyzed. The measured relative error rates are shown in Tables 8 and 9 and Figures 5 and 6. A representative value was set to compare the measurement results according to the presence or absence of the sample from the quasi-steady state temperature data. The reference value set was the U-value measured by the heat flow meter method.

In Case A, the outdoor temperature fluctuations ($\Delta t < 1.0$ °C) in the residential building were constant in Sections (sampled data) 1, 4, and 6. Comparing the results of this section with the representative value, a measured relative error rate of 3.84–5.85% was obtained. The accuracy of the results obtained through data sampling was high. On the contrary, for the data from Sections (sampled data) 2, 3, and 5, where the variation in outdoor temperature was large, the measured relative error rate in the representative value was approximately 12.45–21.84%. The measurement uncertainty that increased when data with large temperature fluctuations were not sampled.

In Case B, the range in the temperature variations were stable in Sections (sampled data) 1 and 5. These data were used to compare the wall U-value and the representative value. The measured relative error rate ranged from 3.39–4.88%; in other words, less than 5%. On the other hand, the error rate range in Sections (sampled data) 2–4, and 6 was 5.47–16.32%.

In Case C, the indoor and outdoor temperature difference ranges were constant in all five sections, and all the results were sampled and analyzed. The measured relative error rate was 4.70%. However, the relative error rate in Sections (sampled data) 1–4, and 6 was relatively large at 7.79–15.59%.

Finally, Case D showed a relative error of at least 3.51% and a maximum of 5.14% in Sections (sampled data) 1, 3, and 6. In sections (sampled data) 2, 4, and 5, where the variations in indoor and outdoor temperatures were relatively large, the measured relative error rate ranged from 6.26–10.94%.

In this study, the U-value was calculated by sampling data at the quasi-steady state, which is a measurement condition under the ASTR method in which there is a very small variation in indoor and outdoor temperature. The measurement accuracy was verified by comparing the measurement results with the results obtained without the sampled data.

As a result, the relative error rate increased when the outdoor temperature fluctuations were greater than 1 °C. This confirms that measurement uncertainty can increase if quasi-steady state conditions are not implemented. The measured relative error rate due to fluctuations in outdoor temperature are shown in detail in Figures 5 and 6.

The measurement results in Sections 4.1 and 4.2 showed a change in the value of U-value at each orientation. The difference in the U-values in the wall direction is analyzed as the cause of the degree of deterioration of wall insulation performance and the measurement error of the sensor. However, the difference in the variance of the fragrant U-value was about 3%, showing no significant difference.

In this study, the energy performance of a building was analyzed by comparing its U-value at initial design and the actual U-value measured in situ. The energy performances of the target buildings were analyzed using Energy Plus Version 8.7, a dynamic energy analysis program. The building input conditions were analyzed with reference to the measured values through energy diagnoses and Kim et al. [45]. As a result, the building energy needs in Case A, B, C, and D increased by 7.9–26.6% compared to the initial design U-value. This difference has a great impact on the energy performance analysis of buildings. Precise in situ wall U-value measurement methods are required to analyze the current energy performance of deteriorated buildings.

The results in Section 4.1 show that the indoor surface side heat transfer coefficient is a factor that can affect the accuracy of ASTR measurement method. In fact, previous studies [35] have shown that the factors affecting the overall heat transfer coefficient in residential buildings depend on the method used in the indoor heating systems.

Table 8. Analysis of measurement results by data sampling.

		U_{ASTR} [W/(m^2·K)]				
Classification	**Item**	**W1 (East)**	**W1 (West)**	**W1 (South)**	**W1 (North)**	**R1**
Case A	U_{HFM}	–	–	1.333	1.328	1.088
	1	–	–	1.277	1.271	1.041
	2	–	–	1.111	1.038	0.888
	3	–	–	1.499	1.508	1.235
	4	–	–	1.278	1.277	1.042
	5	–	–	1.133	1.066	0.901
	6	–	–	1.255	1.258	1.038
Case B	U_{HFM}	–	–	1.81	1.701	1.385
	1	–	–	1.733	1.633	1.338
	2	–	–	1.551	1.488	1.159
	3	–	–	1.601	1.522	1.225
	4	–	–	1.699	1.59	1.288
	5	–	–	1.725	1.618	1.322
	6	–	–	1.711	1.607	1.277
Case C	U_{HFM}	2.155	2.148	2.121	2.266	1.578
	1	1.855	1.832	1.822	1.922	1.332
	2	2.366	2.328	2.325	2.478	1.732
	3	1.975	1.948	1.909	2.082	1.444
	4	1.983	1.955	1.911	2.088	1.455
	5	2.058	2.048	2.018	2.153	1.511
	6	1.933	1.922	1.905	2.023	1.405
Case D	U_{HFM}	1.555	1.508	1.511	1.519	1.055
	1	1.479	1.445	1.435	1.455	1.002
	2	1.388	1.343	1.355	1.345	0.956
	3	1.492	1.433	1.458	1.458	1.008
	4	1.442	1.407	1.408	1.399	0.988
	5	1.441	1.401	1.399	1.401	0.989
	6	1.475	1.443	1.438	1.444	1.001

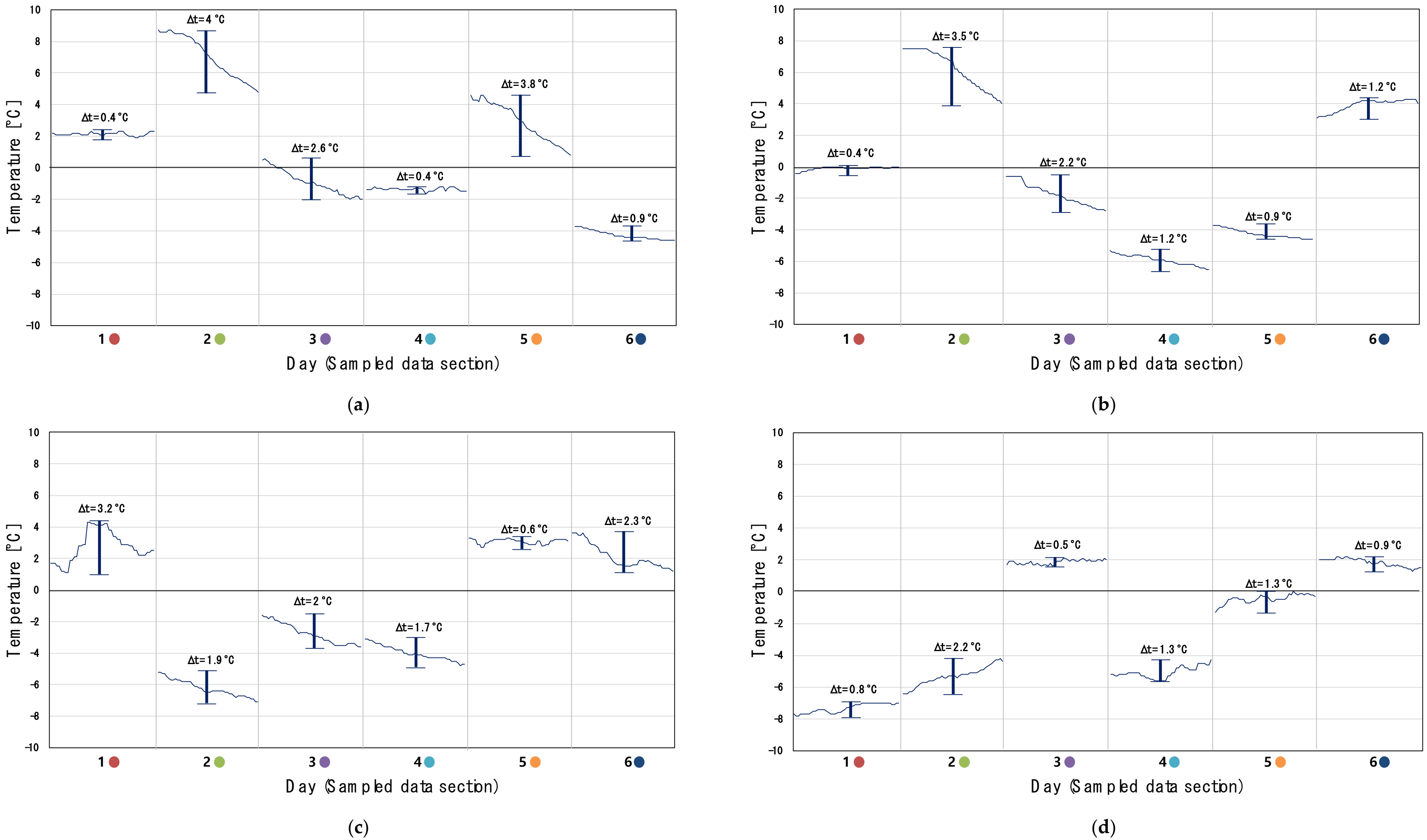

Figure 5. Changes in outdoor temperature: (**a**) Case A; (**b**) Case B; (**c**) Case C; (**d**) Case D.

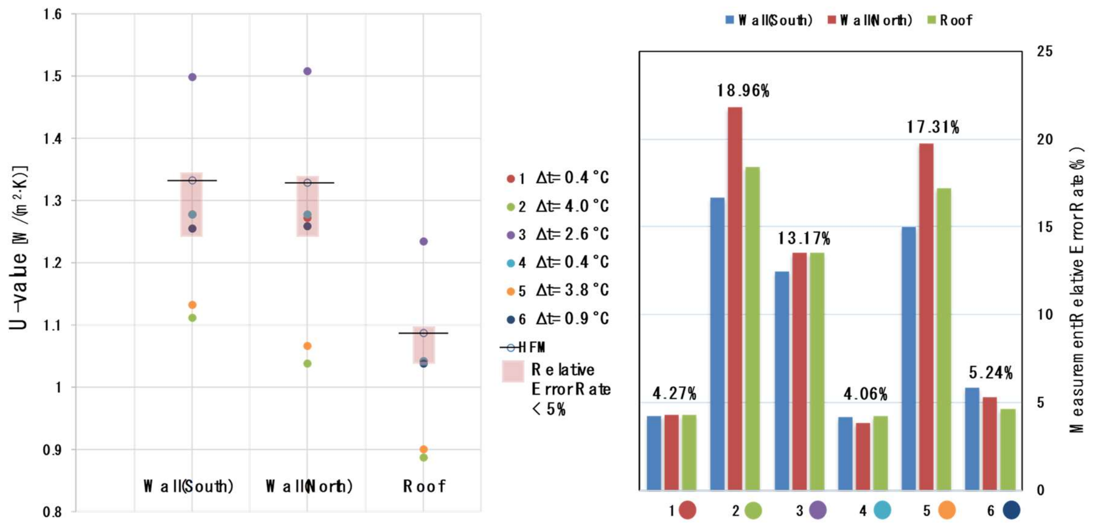

(**a**)

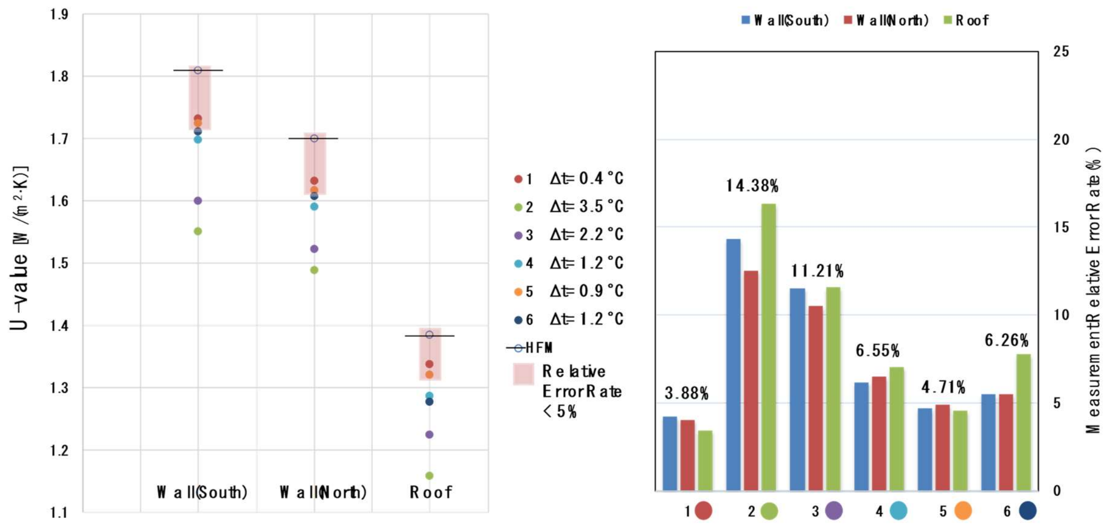

(**b**)

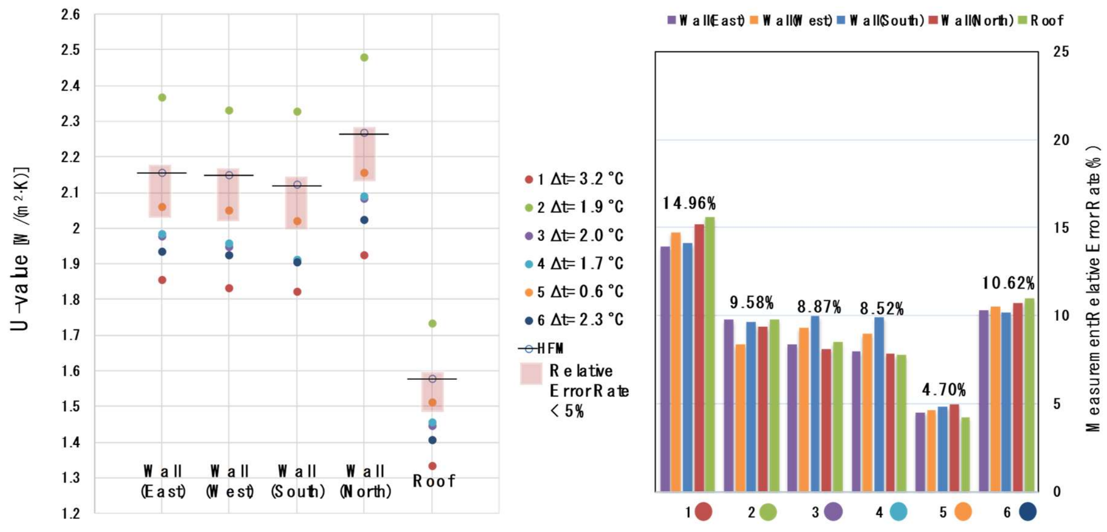

(**c**)

Figure 6. *Cont.*

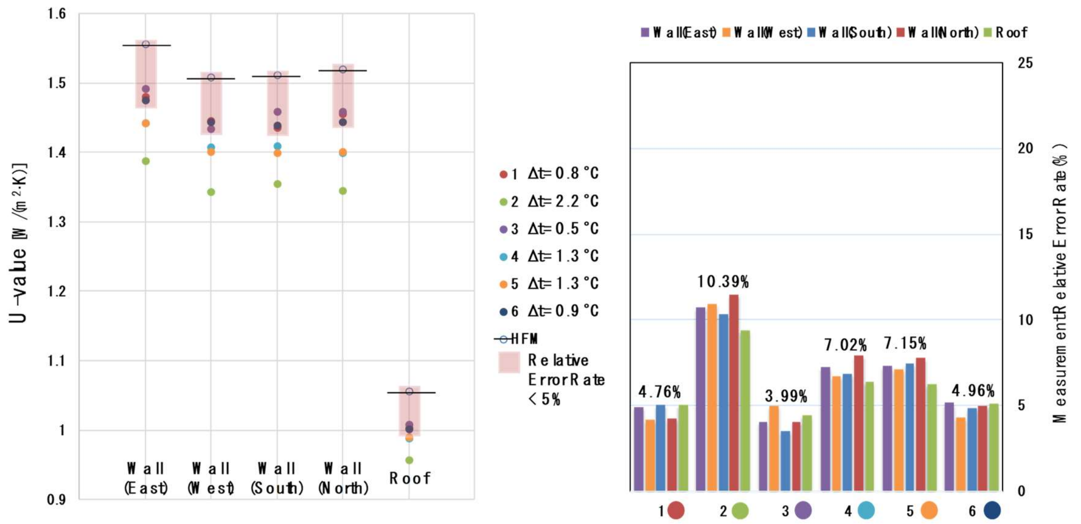

(**d**)

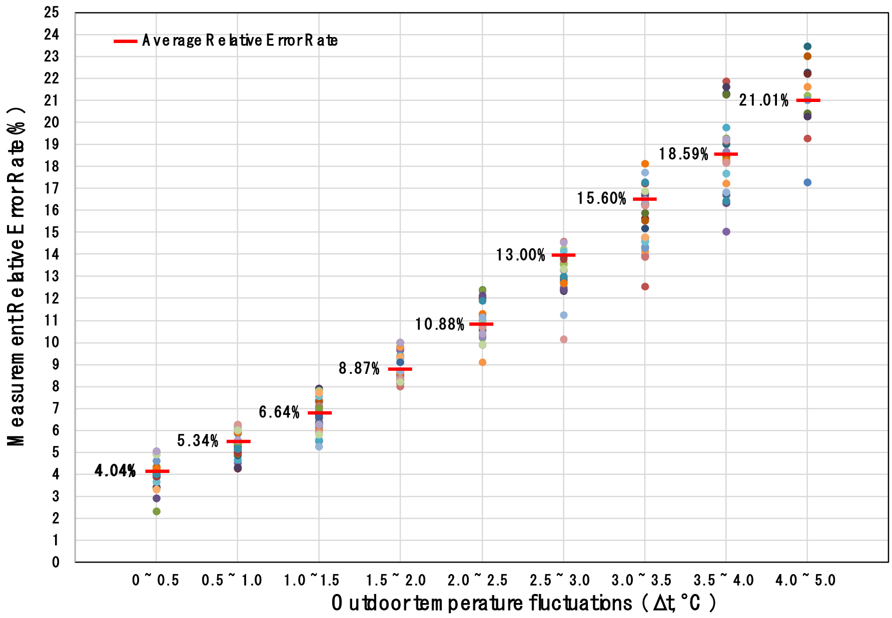

Figure 6. Relative error rate as a function of outdoor temperature fluctuation: (**a**) Case A; (**b**) Case B; (**c**) Case C; (**d**) Case D.

The reason for this difference is the result of the criteria proposed by different countries, derived from their own climate characteristics and indoor heating systems (convection-type heating equipment, radiators). Therefore, there was a difference between these and the value measured in the residential buildings using the Korean floor radiant heating system (Ondol system).

In this study, it was confirmed that the U-value is underestimated or overestimated when the indoor surface heat transfer coefficient values given in the respective standards [1,17] are used. These factors can increase the measurement uncertainty. Therefore, studies are required to measure the indoor total surface heat transfer coefficient using the floor radiant heating system, which is the Korean residential building heating system. Reliable data may be obtained when the U-value is measured by applying the indoor heat transfer coefficient on indoor surfaces.

The results in Section 4.2 showed that fluctuations in outdoor temperature are factors influencing the accuracy of ASTR measurement methods. This confirmed that measurement uncertainty can increase if quasi-steady state conditions are not met. The conditions for increasing the measurement accuracy of the ASTR method are as follows. First, the quasi-steady state measurement condition should be established and a constant room temperature of 20 °C needs to be maintained. Second, it is necessary to conduct the measurement when fluctuations in the outside air temperature are low; reliable data can be obtained when this value is less than 1 °C. Finally, future research will need to analyze the data acquisition algorithm and calculation logic that can sample quasi-steady state section.

Table 9. Relative error rate in the presence or absence of sampled data.

		Relative Error Rate (%)				
Classification		**W1 (East)**	**W1 (West)**	**W1 (South)**	**W1 (North)**	**R1**
Case A	1	–	–	4.20	4.29	4.32
	2	–	–	16.65	21.84	18.38
	3	–	–	12.45	13.55	13.51
	4	–	–	4.13	3.84	4.23
	5	–	–	15.00	19.73	17.19
	6	–	–	5.85	5.27	4.60
Case B	1	–	–	4.25	4.00	3.39
	2	–	–	14.31	12.52	16.32
	3	–	–	11.55	10.52	11.55
	4	–	–	6.13	6.53	7.00
	5	–	–	4.70	4.88	4.55
	6	–	–	5.47	5.53	7.80
Case C	1	13.92	14.71	14.10	15.18	15.59
	2	9.79	8.38	9.62	9.36	9.76
	3	8.35	9.31	10.00	8.12	8.49
	4	7.98	8.99	9.90	7.86	7.79
	5	4.50	4.66	4.86	4.99	4.25
	6	10.30	10.52	10.18	10.72	10.96
Case D	1	4.89	4.18	5.03	4.21	5.02
	2	10.74	10.94	10.32	11.45	9.38
	3	4.05	4.97	3.51	4.02	4.45
	4	7.27	6.70	6.82	7.90	6.35
	5	7.33	7.10	7.41	7.77	6.26
	6	5.14	4.31	4.83	4.94	5.12

5. Conclusions

This study investigated the feasibility of improving the in situ measurement accuracy of the ASTR (air-surface temperature ratio) method. This study also developed a metering system that uses ASTR methods to measure U-values in a simple, fast, and low cost manner. The system was applied to compare the U-values derived from ISO 9869-1 HFM (heat flow meter) and ASTR methods and analyzed the method for obtaining a reliable U-value using the latter.

Firstly, the U-value was calculated by applying standard vertical and horizontal indoor total surface heat transfer coefficients (Korean Energy Design Standard and ISO 6946). The measurement results were derived according to each criterion. The measured relative error rate and accuracy were then compared by using the measurement results. Secondly, the measurement results of sampled data were compared. The U-value was calculated by sampling the quasi-steady state data, which is the most important measurement condition in the ASTR method. The effect of sampling on the measurement (relative error rate) was analyzed.

The indoor total surface heat transfer coefficient was analyzed in two cases using the Korean Energy Saving Design standard and the ISO 6946 standard. The measured relative error rate was analyzed by comparing the results obtained with the HFM method. It was confirmed that the U-value can be underestimated or overestimated according to the value of the indoor surface heat transfer coefficient given in each standard, and that this is a factor that increases the uncertainty of the measured in situ U-value. Therefore, it is necessary to develop a method to improve the accuracy of the ASTR method by calculating the total surface heat transfer coefficient of the envelope of buildings that have a floor radiant heating system, which is mostly seen in domestic residential buildings.

Furthermore, the measurement accuracy was verified by comparing the results obtained through data sampling with those obtained without data sampling. Results show that if the quasi-steady state condition is not implemented, the measurement uncertainty can increase significantly. Therefore, sampling the data under the quasi-steady state measurement condition is the method by which to improve the accuracy of the ASTR method. To realize this quasi-steady state, it is necessary to maintain a constant room temperature. It is also necessary to measure fluctuations in the outdoor temperature on a day when this variation is low. In addition, the measurement accuracy of the ASTR method can be improved by sampling and analyzing data satisfying the quasi-steady state conditions.

Author Contributions: S.-H.K. designed and performed the experiments; J.-H.L. analyzed the data; J.-H.K. conceived the concept of this research, coordinated the study, and finalized the manuscript; H.-G.J. and S.-H.Y. performed, corrected, and analyzed the measurement results and wrote the paper.

Funding: This research received no external funding.

Acknowledgments: This work was supported by the Korea Institute of Energy Technology Evaluation and Planning (KETEP) and the Ministry of Trade, Industry & Energy (MOTIE) of the Republic of Korea (No. 20162010104330).

Conflicts of Interest: The authors declare no conflict of interest.

References

1. Ministry of Land, Infrastructure and Transport (MOLIT). *Amendment of Energy Saving Design Standards for Buildings*; Ministry of Land, Infrastructure and Transport: Sejong-si, Korea, 2017.
2. European Parliament and Council. *Directive 2012/27/EU of the European Parliament and of the Council*; EUR-Lex Access to European Union Law; European Parliament and Council: Brussel, Belgium, 2012.
3. Dall'O, G.; Sarto, L.; Panza, A. Infrared screening of residential buildings for energy audit purposes: Results of a field test. *Energies* **2013**, *6*, 3859–3878. [CrossRef]
4. Kim, S.G.; Kwon, S.W. The study of optimum method about the design and operating through a zero-energy house built in the existing building. *New Renew. Energy* **2015**, 1149–1159. [CrossRef]
5. Korea Energy Economics Institute. *Residential Building Energy Efficiency Improvement Strategy*; Korea Energy Economics Institute: Ulsan, Korea, 2013.
6. Jones, P.; Li, X.J.; Perisolgou, E.; Patterson, J. Five energy retrofit houses in South Wales. *Energy Build.* **2017**, *154*, 335–342. [CrossRef]
7. Elsharkawy, H.; Rutherford, P. Energy-efficient retrofit of social housing in the UK: Lessons learned from a Community Energy Saving Programme (CESP) in Nottingham. *Energy Build.* **2018**, *172*, 295–306. [CrossRef]
8. International Organization for Standardization. *Thermal Insulation—Building Elements—In-Situ Measurement of Thermal Resistance and Thermal Transmittance—Part 1: Heat Flow Meter Method*; ISO Standard 9869-1; International Organization for Standardization: Geneva, Switzerland, 2014.
9. Deconick, A.-H.; Roels, S. Comparison of characterisation methods determining the thermal resistance of building components from onsite measurements. *Energy Build.* **2016**, *130*, 309–320.
10. Shin, M.-S.; Rhee, K.-N.; Yu, J.-Y.; Jung, G.-J. Determination of equivalent thermal conductivity of window spacers in consideration of condensation prevention and energy saving performance. *Energies* **2017**, *10*, 717. [CrossRef]
11. Oh, J.H.; Yoo, H.J.; Kim, S.S. Evaluation of strategies to improve the thermal performance of steel frames in curtain wall systems. *Energies* **2016**, *9*, 1055. [CrossRef]
12. Ficco, G.; Iannetta, F.; Ianniello, E.; Alfano, F.R.d.A.; Dell'Isola, M. U-value in situ measurement for energy diagnosis of existing buildings. *Energy Build.* **2015**, *104*, 108–121. [CrossRef]
13. Cesaratto, P.G.; Carli, D.M. A measuring campaign of thermal conductance in situ and possible impacts on net energy demand in buildings. *Energy Build.* **2013**, *59*, 29–36. [CrossRef]
14. Pisello, A.L.; Cotana, F.; Nicolini, A.; Buratti, C. Effect of dynamic characteristics of building envelope on thermal-energy performance in winter conditions: In field experiment. *Energy Build.* **2014**, *80*, 218–230. [CrossRef]

15. Cheng, X.; Kato, S.; Hiyama, K.; Sihwan, L. The Technological Investigation of Wall Thermal Performance Diagnosis. *Seisan Kenkyu* **2013**, *65*, 5–7.
16. Walker, R.; Pavía, S. Thermal performance of a selection of insulation materials suitable for historic buildings. *Build. Environ.* **2015**, *94*, 155–165. [CrossRef]
17. International Organization for Standardization. *Building Components and Building Elements—Thermal Resistance and Thermal Transmittance—Calculation Method*; ISO Standard 6946; International Organization for Standardization: Geneva, Switzerland, 2007.
18. International Organization for Standardization. *Building Materials and Products—Procedures for Determining Declared and Design Thermal Values*; ISO Standard 10456; International Organization for Standardization: Geneva, Switzerland, 1999.
19. Albatici, R.; Tonelli, A.M. Infrared thermovision technique for the assessment of thermal transmittance value of opaque building elements on site. *Energy Build.* **2010**, *42*, 2177–2183. [CrossRef]
20. Lucci, L. Applications of the infrared thermography in the energy audit of buildings: A review. *Renew. Sustain. Energy Rev.* **2018**, *82*, 3077–3090. [CrossRef]
21. Fokaides, P.A.; Kalogirou, S.A. Application of infrared thermography for the determination of the overall heat. *Appl. Energy* **2011**, *88*, 4358–4365. [CrossRef]
22. Tejedor, B.; Casals, M.; Gangolells, M. Assessing the influence of operating conditions and thermophysical properties on the accuracy of in-situ measured U-values using quantitative internal infrared thermography. *Energy Build.* **2018**, *171*, 64–75. [CrossRef]
23. International Organization for Standardization. *Thermal Insulation—Building Elements—In-Situ Measurement of Thermal Resistance and Thermal Transmittance—Part 2: Infrared Method for Frame Structure Dwelling*; ISO 9869-2; International Organization for Standardization: Geneva, Switzerland, 2017.
24. Ballarini, I.; Corgnati, S.P.; Corrado, V. Use of reference buildings to assess the energy saving potentials of the residential building stock: The experience of TABULA project. *Energy Policy* **2014**, *68*, 273–284. [CrossRef]
25. Albatici, R.; Tonelli, A.; Chiogna, M. A comprehensive experimental approach for the validation of quantitative infrared thermography in the evaluation of building. *Appl. Energy* **2015**, *141*, 218–228. [CrossRef]
26. Lucchi, E. Thermal transmittance of historical brick masonries: A comparison among standard data, analytical calculation procedures, and in situ heat flow meter measurements. *Energy Build.* **2017**, *134*, 171–184. [CrossRef]
27. Kim, S.; Kim, J.; Lee, J.; Jeong, H.; Song, K. Reliability field test on air-surface temperature ratio method for in situ measurement of U-value. *Energies* **2018**, *11*, 803. [CrossRef]
28. Bienvenido-Huertas, D.; Rodriguez-Alvaro, R.; Jose Moyano, J.; Rico, F.; Marin, D. Determining the U-value of facades using the thermometric method: Potentials and limitations. *Energies* **2018**, *11*, 360. [CrossRef]
29. Holman, J.P. *Heat Transfer*, 10th ed.; Department of Mechanical Engineering of the Southern Methodist University: Dallas, TX, USA, 2010.
30. Peng, C.; Wu, Z. In situ measuring and evaluating the thermal resistance of building construction. *Energy Build.* **2008**, *40*, 2076–2082. [CrossRef]
31. Wang, F.; Wang, D.; Wang, X.; Yao, J. A data analysis method for detecting wall thermal resistance considering wind velocity in situ. *Energy Build.* **2010**, *42*, 1647–1653. [CrossRef]
32. Obyn, S.; Moeseke, G. Variability and impact of internal surfaces convective heat transfer coefficients in the thermal evaluation of office buildings. *Appl. Therm. Eng.* **2015**, *87*, 258–272. [CrossRef]
33. Desogus, G.; Mura, S.; Ricciu, R. Comparing different approaches to in situ measurement of building components thermal resistance. *Energy Build.* **2011**, *43*, 2613–2620. [CrossRef]
34. Korea Energy Agency. *Building Energy Saving Plan*; Korea Energy Agency: Seoul, Korea, 2018.
35. Cholewa, T.; Rosinski, M.; Spik, Z.; Dudzinska, R.M.; Siuta-Olcha, A. On the heat transfer coefficients between heated/cooled radiant floor and room. *Energy Build.* **2013**, *66*, 599–606. [CrossRef]
36. Kim, J.; Lee, J.; Jang, C.; Song, D.; Yoo, S.; Kim, J. Heating Energy Saving and Cost Benefit Analysis According to Low-Income Energy Efficiency Treatment Program—Case Study for Low-Income Detached Houses Energy Efficiency Treatment Program. *KIEAE* **2016**, *10*, 39–45. [CrossRef]
37. Lee, J.; Kim, S.; Kim, J.; Song, D.; Jeong, H. Thermal performance evaluation of low-income buildings based on indoor temperature performance. *Appl. Energy* **2018**, *221*, 425–436. [CrossRef]
38. Ryu, Y.; Park, M.; Kim, J.; Joo, H. *A Study on Rural House Remodeling for Improvement of Energy Performance*; Korean Rural Community Corporation: Naju-si, Korea, 2013.

39. Cesaratto, P.; Carli, M.; Marinetti, S. Effect of different parameters on the in situ thermal conductance evaluation. *Energy Build.* **2011**, *43*, 1792–1801. [CrossRef]
40. Ghazi, K.; Binder, B.; Vonbank, R. A simple method to determine the specific heat capacity of thermal insulations used in building construction. *Energy Build.* **2003**, *35*, 413–415. [CrossRef]
41. Rassoli, A.; Itard, L.; Ferreira, C. A response factor-based method for the rapid in-situ determination of wall's thermal resistance in existing buildings. *Energy Build.* **2016**, *119*, 51–61. [CrossRef]
42. Feuermann, D. Measurement of envelope thermal transmittances in multifamily buildings. *Energy Build.* **1989**, *13*, 139–148. [CrossRef]
43. Trethowen, H. Measurement errors with surface-mounted heat flux sensors. *Energy Build.* **1986**, *21*, 41–56. [CrossRef]
44. International Organization for Standardization. *Thermal Insulation—Qualitative Detection of Thermal Irregularities in Building Envelopes—Infrared Method*; ISO Standard 6781; International Organization for Standardization: Geneva, Switzerland, 1983.
45. Kim, S.; Kim, J.; Lee, J.; Jeong, H.; Song, K. The method of in-situ ASTR method diagnosing wall U-value in existing deteriorated houses. *KIEAE* **2017**, *8*, 41–48. [CrossRef]